

# Wavelength Calibration of the VLT-UVES Spectrograph

Jonathan B. Whitmore<sup>1</sup>, Michael T. Murphy<sup>2</sup>, and Kim Griest<sup>1</sup>,  
 jonathan.b.whitmore@gmail.com, mmurphy@swin.edu.au, kgriest@ucsd.edu

## ABSTRACT

We attempt to measure possible miscalibration of the wavelength scale of the VLT-UVES spectrograph. We take spectra of QSO HE0515-4414 through the UVES iodine cell which contains thousands of well calibrated iodine lines and compare these lines to the wavelength scale from the standard Thorium-Argon pipeline calibration. Analyzing three exposures of this  $z = 1.71$  QSO, we find that there are average wavelength calibration shifts between 100 m/s and 500 m/s depending upon the exposure. Within a given exposure and even within a given echelle order we find shifts of 100 m/s up to 200 m/s. These calibration errors are similar to, but smaller than, those found earlier in the Keck HIRES spectrometer. We also explore the implications of these calibration errors on the systematic error in measurements of  $\frac{\Delta\alpha}{\alpha}$ , the change in the fine structure constant derived from accurate measurement of the relative redshifts of absorption lines in QSO absorption systems. Using either our measured calibration offsets or a Gaussian model with sigma of around 90 m/s, Monte Carlo mock experiments find errors in  $\frac{\Delta\alpha}{\alpha}$  of between  $1 \times 10^{-6} N_{\text{sys}}^{-1/2}$  and  $3 \times 10^{-6} N_{\text{sys}}^{-1/2}$ , where  $N_{\text{sys}}$  is the number of systems used and the range is due to dependence on how many metallic absorption lines in each system are compared.

## 1. Introduction

In a recent paper (Griest et al. 2010) it was shown that Keck HIRES spectrograph measurements of emission features in high redshift QSOs calibrated by the normal Thorium-Argon (Th/Ar) pipeline contained overall shifts between exposures of up to 2000 m/s over several nights and errors of up to 500 m/s even within a single order in a single exposure. Similar wavelength calibration problems were found previously by Osterbrock, et. al (2000), and Suzuki, et al. (2003). These results were found by re-calibrating the wavelength scale using spectra taken through the Keck HIRES iodine cell. The iodine cell, which has been used extensively in the Doppler method search for extrasolar planets, puts several sharp lines per Angstrom on top of the QSO spectrum, and its reproducible absorption spectrum allows extra-solar planet workers to attain a relative ve-

locity precision of around 1 m/s between exposures taken up to several years apart.

For most astronomical work wavelength calibration errors of around 1 km/s are not important, but over the past few years several groups have used absorption lines in the spectra of high redshift QSOs to measure or place limits on possible changes in the fine structure constant over cosmological time. If the fine structure constant was different 10 billion years ago by the claimed detection of  $\frac{\Delta\alpha}{\alpha} = (-5.43 \pm 1.16) \times 10^{-6}$  (Murphy, et al. 2003, 2004), relative atomic transition wavelengths are expected to differ from their lab values by up to 100 m/s. For such experimental uses it is important to pay careful attention to calibration errors of the size reported above. However, it is important to understand that while individual measurement errors may be larger than the expected signal, if many atomic transitions are used in many QSO absorption systems, it may be possible to average away these calibration uncertainties. See for example Murphy, et al. (2009).

The results of Griest et al. (2010) apply only

<sup>1</sup>Department of Physics, University of California, San Diego, CA 92093, USA.

<sup>2</sup>Swinburne Univ. Melbourne, Australia

to the Keck HIRES instrument, but there is another instrument, the VLT UVES spectrograph, that is playing a key role in the search for possible changes in the fine structure constant using absorption lines in high redshift QSOs. In this paper we perform a similar re-calibration of the standard UVES Th/Ar wavelength calibration pipeline using the VLT iodine cell. We find similar, but smaller, wavelength calibration errors. We also make a first attempt at calculating whether these calibration errors can give rise to important systematic errors in the measurements to date of  $\frac{\Delta\alpha}{\alpha}$ .

There has been considerable controversy in experimental measurements of  $\frac{\Delta\alpha}{\alpha}$  using high redshift absorption systems, with claims of detection and also limits on variation inconsistent with those claims. See Murphy, et al. (2008) for a summary.

## 2. Observations

Six exposures were taken of the quasar HE0515-4414 ( $z=1.71$ ) with the VLT UVES spectrograph in October 2003. In this paper we analyze the wavelength calibration of the three exposures that were taken with the iodine cell in place. We first note that ESO’s specifications for UVES are that the gratings, after being moved, be returned to the same position to within a tolerance corresponding to 0.1 pixels (D’Odorico, et al. 2000). Thus naively we might expect to see an overall non-zero velocity calibration shift between the iodine and Th/Ar lines of roughly 140 m/s at 5500 Å. The six QSO exposures were taken during two nights, with the first two I<sub>2</sub> QSO exposures being taken on the first night and the third I<sub>2</sub> exposure taken on the next. The first two exposures were calibrated with the same Th/Ar exposure; however we note that the gratings were moved after the two data exposures and then moved back to the same position in order to take the ThAr exposure. The third I<sub>2</sub> QSO exposure was followed first by a non-I<sub>2</sub> QSO exposure (same QSO, grating setting, etc.) and then by the Th/Ar calibration exposure. We had hoped this scheduling would remove a possible source of error caused by grating movement, but in fact, the third QSO I<sub>2</sub> exposure was part of a different “observation block”, meaning the gratings were reset (moved and then returned) between the data and Th/Ar exposures.

## 3. Data Analysis

The UVES spectra were extracted using the standard UVES Common Pipeline Language (CPL) software package which does wavelength calibration using Th/Ar lamp exposures taken at times given in Table 2. Rather than co-adding exposures, we treated each of the three exposures separately, so each I<sub>2</sub> (and accompanying Th/Ar) exposure gives a separate measurement of the Th/Ar wavelength calibration shift.

To perform the wavelength recalibration using the iodine lines we used a method similar to that used in Griest, et al. (2010). A well measured iodine cell absorption spectrum taken elsewhere is convolved with a Gaussian to give it the same resolution as the iodine lines in our QSO spectra. It is then multiplied by an overall normalization and shifted in wavelength by an amount that gives the smallest possible  $\chi^2$  in the difference between the convolved iodine spectrum and the QSO spectra. Care is taken in the continua fitting as discussed in Griest, et al. (2010), since the iodine lines cover nearly the entire spectrum. For the reference iodine spectra we tried both the Marcy and Butler (Butler, et al., 1996; Marcy, 2008) FTS spectrum of the Keck HIRES iodine cell done at KPNO with a resolving power,  $R = 170,000$  and a signal/noise of 700 per pixel, and the UVES iodine cell calibration spectrum,<sup>1</sup> performed at 70°C, with a spectral resolution 0.020 cm<sup>-1</sup> (which implies  $R > 1,000,000$  throughout the effective I<sub>2</sub> wavelength range). Besides the difference in resolution and a single shift in the absolute scale, the resulting calibration shifts were fairly similar using the two different reference spectra. For UVES iodine cell data it is clearly more appropriate to use the UVES FTS iodine cell spectrum so we will only present results obtained using this spectrum.

## 4. Results

The result of our analysis is a wavelength offset between the iodine cell value, which is presumed to be correct, and the Th/Ar value output by the standard UVES pipeline software. In fact, it is not important to our work that the FTS iodine spectrum be absolutely correct, since we only care about relative shifts across an individual ex-

<sup>1</sup>[www.eso.org/sci/facilities/paranal/instruments/uves/tools](http://www.eso.org/sci/facilities/paranal/instruments/uves/tools)

TABLE 1  
JOURNAL OF OBSERVATIONS

Exposure and Date	Time (UT)	ThAr Time (UT)
1 2003-10-11	07:32	10:56
2 2003-10-11	08:13	10:56
3 2003-10-13	05:31	07:06

posure, and perhaps shifts over time. The iodine cell provides a highly repeatable calibration spectrum whose relative wavelength precision should be better than HIRES or UVES spectra because it stems from laboratory Fourier transform spectra.

The fit for calibration offset is affected by the size of the wavelength bin used in the comparison, with a larger bin giving a smaller formal fit error but less resolution on the wavelength scale over which calibration errors occur. As a compromise we use a bin of 350 km/s or 6Å at 5500Å. We translate these wavelength calibration shifts into velocity using  $v_{\text{shift}} = c \times \Delta\lambda/\lambda$  and display the result for each exposure in Figure 1.

We considered each order from each iodine exposure separately. We began by continuum fitting the exposure and masking the data that falls under strong quasar absorption lines and data near the edges of the order where signal/noise dropped  $< 8$  per pixel. Considering the remaining data as one large wavelength bin, we performed a simultaneous fit for three variables: the overall normalization multiplication factor to the continuum, the Gaussian convolution kernel, and the overall wavelength shift. The wavelength offset found this way is in some sense the average offset for the entire order. We then held the Gaussian convolution sigma and normalization factor fixed for the whole order and fit for the wavelength calibration shifts in the smaller wavelength bins across the order. These smaller bins are roughly centered on each data point, giving a value at each wavelength with the effect of a smoothing filter of 350 km/s.

One sees from Figure 1 that there are constant relative wavelength calibration shifts between exposures from around 100 m/s up to around 500 m/s. These are similar to, but smaller than, the wavelength calibration errors found in the Keck

HIRES iodine data (Griest, et al. 2010). The echelle orders overlap somewhat in wavelength coverage, so we alternate blue and black to show the change of order. The red solid dots, which are the “average” shifts for each order, also show this. Note that we, in addition, find relative calibration shifts within each order of each exposure of typically 100 m/s, and occasionally as high as 500 m/s, again with a pattern similar to, but smaller in amplitude than, HIRES. Finally, again similar to Keck HIRES, we see fairly large shifts as a function of time. Exposures 1 and 2 have an average shift of around 100 m/s, while exposure 3, taken on the next day is off by about 500 m/s. Note that for all three exposures, the echelle gratings were moved between the Th/Ar exposure and the data exposure. It is interesting that while the more finely binned shifts vary substantially across the entire wavelength range, the average shifts of each order (shown by the red solid dots) are quite constant across the entire wavelength range. There thus seems to be a small scale intra-order wavelength calibration shift within each echelle order whose shape is similar for each order, laid on top of a fairly large overall constant shift from zero that depends on only the exposure (and which could be caused by grating shifts, temperature/pressure drifts, etc. between I<sub>2</sub> and Th/Ar exposures.) We will explore the constancy of the intra-order shift across orders below.

A way of seeing the importance of these shifts is to plot the shift distribution. This is shown in Figure 2 which is just a histogram of the shifts for each of the exposures. The shift from each fine wavelength bin is given equal weight in the figure, which, if normalized, can therefore be interpreted as a sort of probability of finding a shift of that value. We use this histogram in this way below when we investigate the effect these shifts might

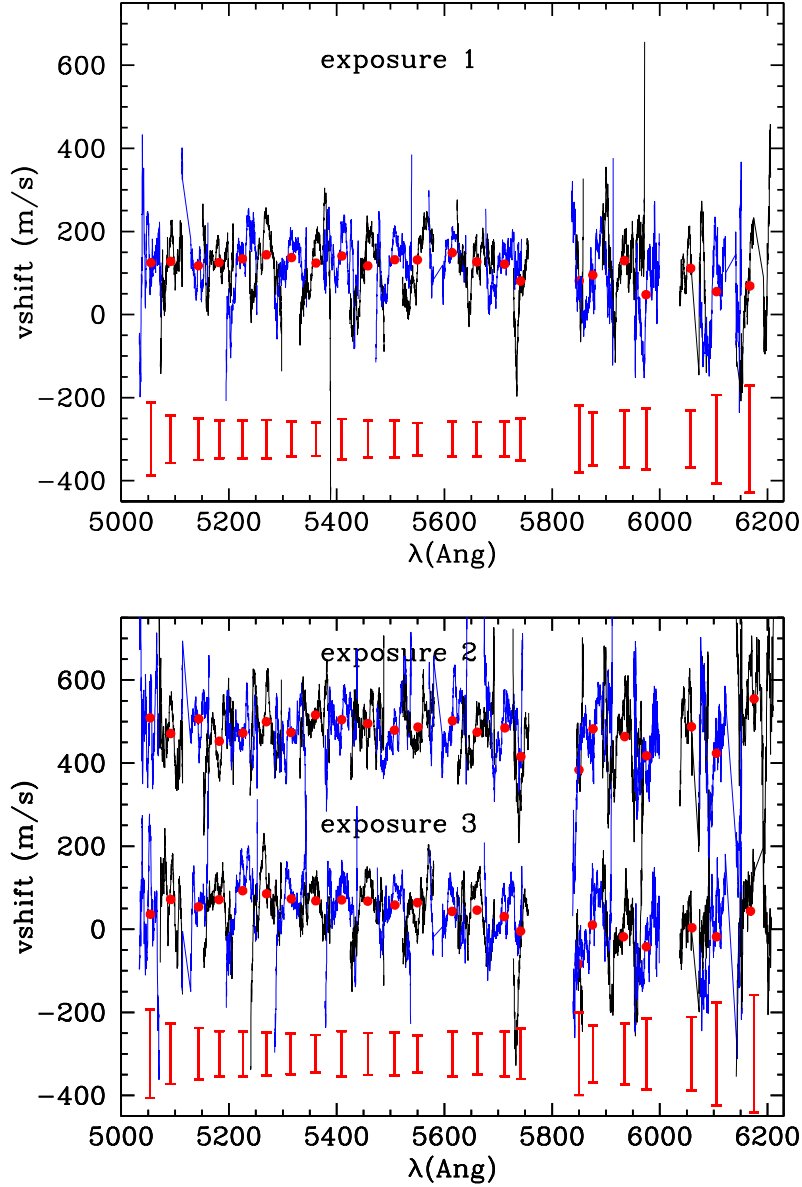


Fig. 1.— The shift in m/s needed to bring the Th/Ar VLT UVES calibration in line with the iodine spectrum. The top figure shows all orders of exposure 1, with blue and black colors alternating for each echelle order. The red dots show the shift needed to bring the entire order in line with the iodine spectrum (similar to the average correction for each order). The red error bars near the bottom show the 1-sigma error in the red dots, and can be used to estimate the uncertainty in each data point. The bottom shows the same for exposure 2 and exposure 3. Note shifts with  $\lambda < 5800\text{\AA}$  are from the lower chip, ‘l’, while the shifts with  $\lambda > 5800\text{\AA}$  are for the upper chip ‘u’.

have on measurements of  $\frac{\Delta\alpha}{\alpha}$ . Of course the shift values for nearby pixels are strongly correlated due to our smoothing, but this is not important for how we use these distributions below. We note that exposure 1 has a mean calibration shift of 112 m/s with a standard deviation of 81 m/s, exposure 2 has a mean of 30 m/s with sigma 91 m/s, and exposure 3 has mean 480 m/s and sigma 86 m/s.

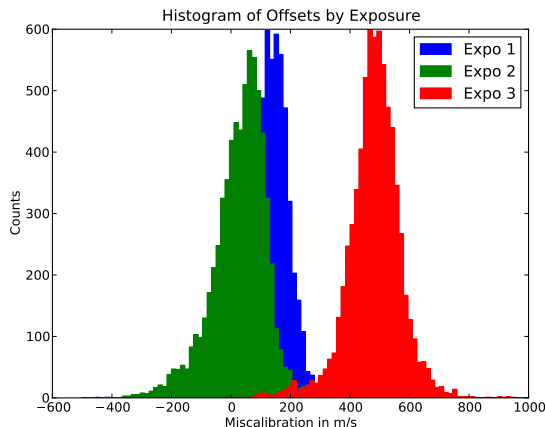


Fig. 2.— Histograms of shifts from the three I<sub>2</sub> exposures Exposure 1 is plotted in blue (in the middle), exposure 2 in green (on the left) and exposure 3 in red (on the right).

Next, as pointed out by Murphy, et al. (2009), an overall velocity shift in a given spectrum should not matter much since it is the comparison between lines that give  $\frac{\Delta\alpha}{\alpha}$ , and if they all shift together it may not matter how large that shift is:

$$\Delta\alpha/\alpha \propto \Delta v_{ij}/c \quad (1)$$

where  $\Delta v_{ij}$  is the velocity shift *between* two lines, *i* and *j*. So it is the shifts within a single exposure that are expected to have the most impact on  $\frac{\Delta\alpha}{\alpha}$  determinations. Examination of Figure 1 gives the impression that there is a pattern of offsets that repeats in each echelle order. To test this hypothesis, we overlaid all the echelle orders of each exposure on a common wavelength scale and then averaged them. This provides the average intra-order distortion for a given exposure. We did this separately for each exposure since the distributions of shifts shown in Figure 2 show large variation between the exposures. We also treat the UVES upper, ‘u’, chip orders separately from the

UVES lower, ‘l’, chip orders. Thus we have six figures, labeled Figure 3(a)-(c) and Figure 4(a)-(c).

Examination of these figures shows a weak pattern, but not as convincing as we had hoped would exist. For the ‘u’ chip there is some similarity between all the exposures, Figures 3(a)-(c) showing a rise in  $v_{shift}$  of more than 100 m/s from about 0.4 to 0.7 (40% to 70% through the average echelle order), followed by a drop of around 100 m/s until around 0.8, and then roughly constant to 1.0. However, the first part of the average orders differ substantially between the exposures, with Figures 3(b) and (c) showing calibration decreases of several hundred m/s for the first parts of the order, and exposure 1 showing an increase over the same region. The ‘l’ chip shows more constancy over the entire average order. The same pattern appears as in the ‘u’ chip, but with less amplitude.

The hope was that a strong pattern would obtain that would allow a correction to be made to the Th/Ar calibration. Unfortunately, the differences in patterns between the different exposures mean that a universal correction that could be applied to all exposures is not likely from this effect alone. More work is clearly needed, probably on a larger data set.

## 5. Effect on $\frac{\Delta\alpha}{\alpha}$

As stated in the introduction, wavelength calibration errors of the magnitude presented in this paper are unimportant for most astronomical work. In this section we wish to address the question of whether or not calibration errors such as we are finding can make a difference in experiments looking for changes in  $\frac{\Delta\alpha}{\alpha}$ . In order to proceed we need an estimate of the magnitude of  $\frac{\Delta\alpha}{\alpha}$  we wish to be sensitive to. There are at least two possible sources for this number: first,  $\frac{\Delta\alpha}{\alpha} = (-5.43 \pm 1.16) \times 10^{-6}$ , which is the most robust claimed detection of  $\frac{\Delta\alpha}{\alpha}$  (Murphy, et al. 2001a, 2001b, 2003, 2004). Second there are several claimed limits on  $\frac{\Delta\alpha}{\alpha}$  near  $\frac{\Delta\alpha}{\alpha} < 1 \times 10^{-6}$  (Chand, et al. 2004; Srianand, et al. 2004; Levshakov, et al. 2006, 2007; Molaro, et al. 2008; c.f. Murphy et al. 2008). Thus the question we would like to ask is to see whether the UVES wavelength calibration errors discussed above, alone can give rise to estimates of  $\frac{\Delta\alpha}{\alpha}$  in the  $1 \times 10^{-6}$  to  $5 \times 10^{-6}$  range.

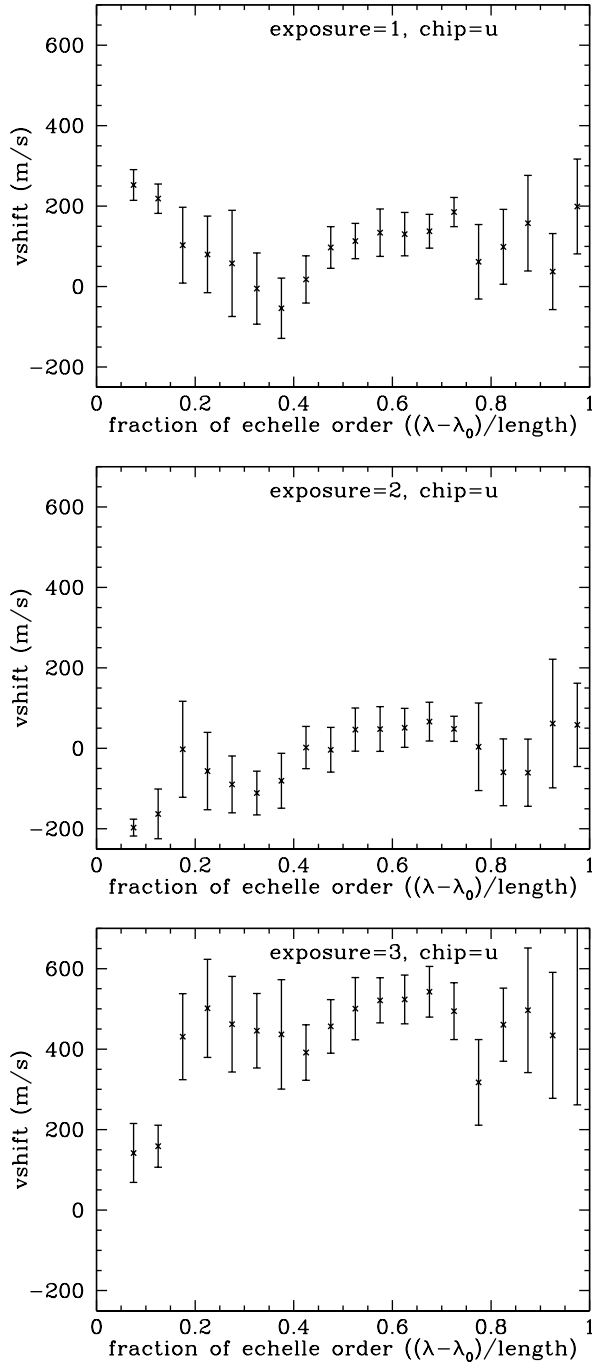


Fig. 3.— Average calibration shifts for the ‘u’ (upper) chip as a function of position within the average echelle order. The wavelength position with the order ranging from 0 to 1 is plotted on the abscissa, while the average calibration shift in m/s at each position bin is plotted on the ordinate. The standard deviation of each calibration shift is plotted as the error bar. The exposure is labeled.

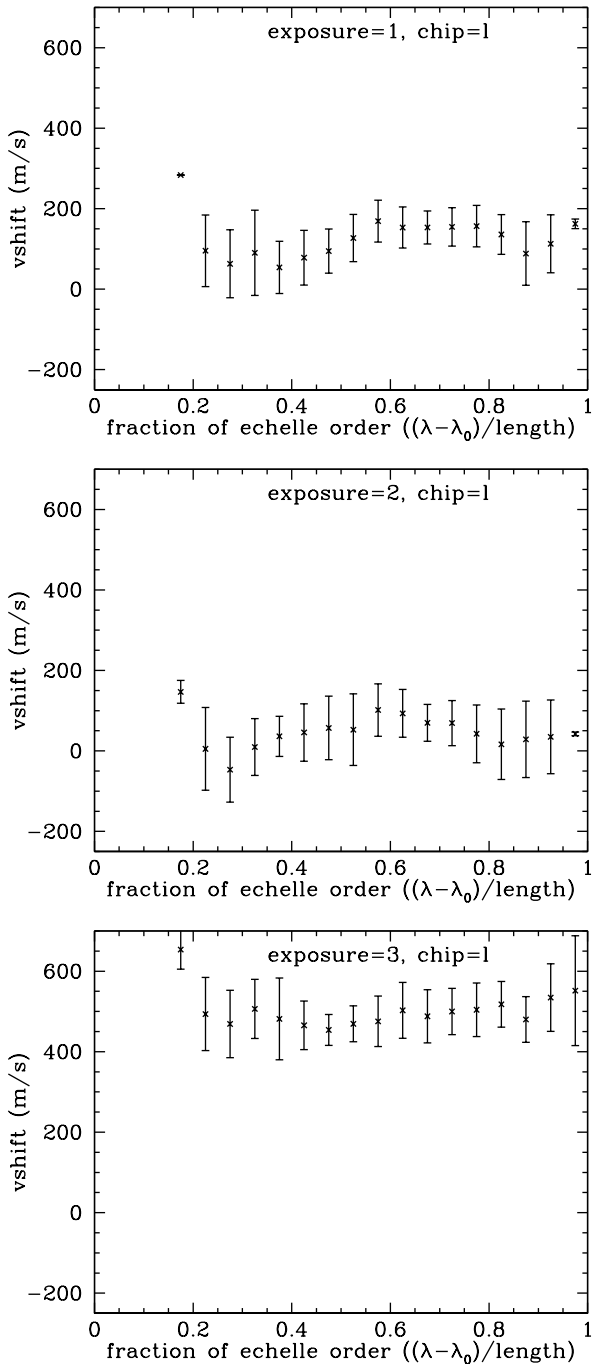


Fig. 4.— Same as last figure, but for the lower ‘l’ chip.

Naively, one might expect the calibration errors of 100 m/s to 500 m/s we found above to give rise to spurious detections of  $\frac{\Delta\alpha}{\alpha}$  of order  $1 \times 10^{-6}$ . If  $\alpha$  was different in the past, the velocity shift of an absorption line from the lab value due changing  $\alpha$  can be found from

$$v_j = v_0 + \left(\frac{\Delta\alpha}{\alpha}\right) x_j, \quad x_j = -2cq_j\lambda_{0j}, \quad (2)$$

where  $j$  numbers the atomic transitions that are being compared,  $v_0$  is a constant offset (degenerate with the system redshift), the  $x_j$  are constants that depend only on the wavelength  $\lambda_0$  of the transition, and the  $q_j$  characterize the sensitivity of each transition to a change in  $\frac{\Delta\alpha}{\alpha}$ . For transitions of interest in QSO absorption work these  $q$ -values range in magnitude from around  $20 \text{ cm}^{-1}$  to  $2000 \text{ cm}^{-1}$  (Porsev, et al. 2007), giving rise to velocity shifts of a few meters per second up to around 100 m/s (for a value of  $\frac{\Delta\alpha}{\alpha} = -5.4 \times 10^{-6}$ ). Thus for individual transitions, the sizes of the wavelength calibration errors found above are of the order of or larger than the sizes of the signal expected from a changing  $\alpha$ .

However, the value of  $\frac{\Delta\alpha}{\alpha}$  obtained does not depend upon just one transition, but is always a comparison of two or more transitions. Thus an overall velocity shift of 500 m/s as seen in exposure 3 above is not relevant as long as comparisons are not done across different exposures. Figure 1 shows that the relative shift across one exposure is substantially smaller than the overall shift. In addition, if the calibration shift error is random, and equally likely to be negative as positive, then it can be removed by averaging over many transitions and many lines of sight. Potential problems do exist if the distribution of shifts is not random, or if the sizes of the errors are large enough that a good measurement requires too many transitions or too many lines-of-sights. Thus we wish to perform some mock experiments using the above distributions of calibration shifts to see what the effect on  $\frac{\Delta\alpha}{\alpha}$  would be.

In an actual experiment, a value of  $\frac{\Delta\alpha}{\alpha}$  is estimated by doing a large joint fit of the the Voigt line profiles, the system redshifts, and the possible velocity offset due to  $\frac{\Delta\alpha}{\alpha}$ . In our Monte Carlo mock experiments we try to calculate a value of  $\frac{\Delta\alpha}{\alpha}$  using the UVES VLT data, but without measuring any actual absorption lines. Instead of us-

ing the fit system redshifts to find velocity offsets, we use the wavelength calibration offsets given in Figure 1, and add these to the lab values of  $\lambda_0$  in Equation 2.

The basic method is as follows. We first choose a random redshift in the range  $z = 0.2$  to  $z = 3.7$ , and calculate the wavelengths of the 23 atomic transitions that were studied in Murphy, et al. (2003). We define  $N_{\text{tran}}$ , the number of these 23 transitions that fall at wavelengths for which we have iodine wavelength calibration. We require at least  $N_{\text{min}}$  transitions, and show our results as a function of this  $N_{\text{min}}$  (a typical value is  $N_{\text{min}} = 4$ , and we do not find any cases with  $N_{\text{tran}} > 9$ ). For each such transition we shift its wavelength by an amount given by one of the exposures in Figure 1. We then perform a fit of Equation 2 for  $\frac{\Delta\alpha}{\alpha}$  and its error. This counts as one absorption system, and we repeat this procedure  $N_{\text{sys}}$  times, averaging the values of  $\frac{\Delta\alpha}{\alpha}$  obtained. We consider values of  $N_{\text{sys}}$  ranging from  $N_{\text{sys}} = 143$ , the number of systems used in Murphy, et al. (2003, 2004), to  $N_{\text{sys}} = 1$ , the value when only one system in one QSO is being analyzed. The above procedure constitutes one Monte Carlo experiment. We repeat the experiment many times to find an average value of  $\frac{\Delta\alpha}{\alpha}$  and its standard deviation (measured by the variance of  $\frac{\Delta\alpha}{\alpha}$  for the many experiments).

We present resulting average values of  $\frac{\Delta\alpha}{\alpha}$  along with their standard deviations as a function of  $N_{\text{sys}}$  and  $N_{\text{min}}$  in Table 2 for 200,000 mock experiments. The table shows results for  $N_{\text{sys}} = 143$  and  $N_{\text{sys}} = 1$ . Note one expects the standard deviation in  $\frac{\Delta\alpha}{\alpha}$  to simply scale as  $N_{\text{sys}}^{-1/2}$ , which is close to what we find in Table 2. Thus, we will use this scaling from now on and only report Monte Carlo experiments for  $N_{\text{sys}} = 1$ .

Besides using the actual wavelength calibration errors above, we also ran several Monte Carlo simulations using two simple models of the calibration offsets. The results of these simple models are also reported in Table 2. For the first model we used a Gaussian random velocity offset with a sigma equal to the exposure 1 velocity standard deviation. For the second, we modeled the velocity offsets as a sine function with amplitude equal to  $\pi/2$  times the standard deviation of the velocity offsets for one of the exposures above, and with a wavelength of about one echelle order. For this case,

we found the results did not depend strongly on the sine wavelength. As seen in Table 2 the results for  $\sigma(\frac{\Delta\alpha}{\alpha})$  are quite similar for all three exposures and for the Gaussian and sine function models.

Table 2 shows several interesting things. First in all cases when  $N_{\min} = 2$ , both the mean calibration offset and sigma in  $\frac{\Delta\alpha}{\alpha}$  are substantially larger than expected from a simple  $1/\sqrt{N_{\text{tran}}}$  scaling. We think this is due to occasional cases where there are very few transitions found, but these lie close together in  $x_j = -2cq_j\lambda_j$ . Since  $\frac{\Delta\alpha}{\alpha}$  is basically the slope in Equation 2, a small  $\Delta x$  offset can result in a very large slope and therefore a large error in  $\frac{\Delta\alpha}{\alpha}$ . It takes just a few such cases to greatly increase the standard deviation. A lesson here may be to not use systems in which very few transitions can be compared. For example, in the alkali doublet method (e.g. Bahcall et al. (1967), Varshalovich, et al. 2000, etc.) two transitions that are close together in wavelength are compared, so this method would be sensitive to intra-order distortions. More generally, even for  $N_{\min} = 4$  and  $N_{\min} = 6$  we find the errors dropping more quickly with  $N$  than  $1/\sqrt{N}$ .

Next we note that the results for all three exposures and for the Gaussian and sine function error models are quite consistent, especially when one takes into account that the standard deviation of velocity offsets for exposure 1 is slightly smaller than for the other exposures. Also as expected the large overall velocity shift for exposure 3 had no effect.

If we restrict ourselves to the  $N_{\min} = 6$  column, and consider  $N_{\text{sys}} = 143$ , we see that the systematic error introduced to a many multiplet measurement of  $\frac{\Delta\alpha}{\alpha}$  is around  $0.28 \times 10^{-6}$ , significantly smaller than the statistical error of  $1.16 \times 10^{-6}$  stated in Murphy, et al. (2003, 2004). We do note that Murphy, et al. (2003, 2004) used the Keck HIRES spectrograph and not the VLT UVES instrument.

An important problem with the above results is that the value of  $\frac{\Delta\alpha}{\alpha}$  and its standard deviation depends strongly on  $N_{\text{tran}}$ , the number of transitions compared in each system, and that no cases were found with  $N_{\text{tran}} > 9$ . This latter fact is because the results above only included lines that overlapped with our iodine cell coverage. Thus  $N_{\text{tran}}$  found in our Monte Carlo experiments are artificially lower than in an actual experiment, which

typically has more spectral coverage. Since the value of  $\sigma(\frac{\Delta\alpha}{\alpha})$  drops quickly with  $N_{\text{tran}}$ , we also expect an actual experiment to find smaller deviations than the ones we report. We find this low value of  $N_{\text{tran}}$  to be especially true for certain values of  $z$ , where very few interesting lines fall within our iodine cell coverage. Our attempt to get around this by setting a minimum number of transitions,  $N_{\min}$ , was partially successful, but Table 2 shows strong dependence on  $N_{\min}$ . Even more clearly we see this in Table 3 where the values of sigma of  $\frac{\Delta\alpha}{\alpha}$  depend on  $N_{\text{tran}}$  substantially more strongly than  $1/\sqrt{N_{\text{tran}}}$ . We note that when  $N_{\text{tran}}$  is specified in the table, exactly  $N_{\text{tran}}$  transitions are compared, while when  $N_{\min}$  is specified all cases that have  $N_{\text{tran}} \geq N_{\min}$  are used.

To remedy this situation we need to somehow estimate the calibration offsets in regions of the spectra where we do not have iodine cell coverage. We attempt to do this by replicating the calibration offsets from the regions where we measure them to all the other spectral regions where interesting transitions occur; i.e. we assume that the distributions of shifts illustrated in Figure 1 apply to all wavelengths. We then repeat the Monte Carlo experiments above.

Results of these simulations are shown in Figure 5 and in Table 4. Now we find few systems with less than 10 transitions and many with around 18. The values of  $\sigma(\frac{\Delta\alpha}{\alpha})$  for low values  $N_{\min}$  are similar to those found in the iodine coverage only Monte Carlos, again depending very strongly on  $N_{\min}$  (or  $N_{\text{tran}}$ ), but for larger values of  $N_{\min}$ ,  $\sigma(\frac{\Delta\alpha}{\alpha})$  stabilizes and approaches the expected,  $1/\sqrt{N_{\text{tran}}}$ , behavior as  $N_{\min}$  increases. We think the high values of  $\sigma(\frac{\Delta\alpha}{\alpha})$  at low  $N_{\min}$  are because for very small  $N_{\text{tran}}$  it is possible to have transitions very close together in  $x = -2cq_j\lambda_{0j}$  that dominate the measurement. Since  $\frac{\Delta\alpha}{\alpha}$  is the slope of the line  $v_j = v_0 + x_j\frac{\Delta\alpha}{\alpha}$ , any error in wavelength calibration is divided by this  $\Delta x$ , giving a large error which will propagate into the mean and especially the standard deviation of  $\frac{\Delta\alpha}{\alpha}$ .

The strong dependence of  $\sigma(\frac{\Delta\alpha}{\alpha})$  on  $N_{\min}$  is interesting and suggests that the standard lore that says it is better to use transitions in the same echelle order, or at least close together in wavelength, may not be true. The wavelength calibration errors we found above exist even within single echelle orders. Thus it may be more robust



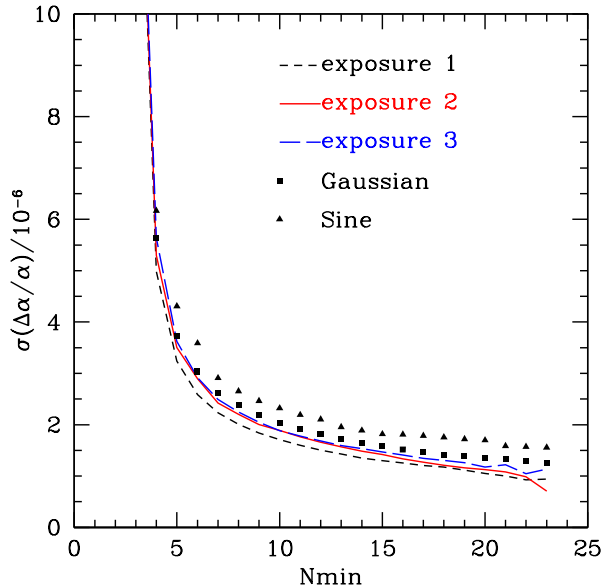


Fig. 5.— Scaling of  $\sigma(\frac{\Delta\alpha}{\alpha})$  with  $N_{\min}$ , the minimum number of transitions allowed in a system. This is for full wavelength coverage between 3000Å and 10500Å, with repeated calibration errors. 200,000 Monte Carlo realizations were used with  $N_{\text{sys}} = 1$ .

to measure or limit  $\frac{\Delta\alpha}{\alpha}$  using transitions that are well separated in  $x$ ; the extra “lever arm” may be advantageous in reducing scatter.

Overall, the large  $\sigma$ 's found at small  $N_{\text{tran}}$  imply that due to wavelength calibration errors it may be dangerous to attempt to measure  $\frac{\Delta\alpha}{\alpha}$  using only a few transitions in one or two systems. Until better understanding is found as to the source of these calibration errors it is probably important to average the errors away by using many transitions in many absorption systems.

We also see from Figure 5 that the mean and standard deviation for all three exposures agree well, and that the three experimentally determined measurements of  $\sigma(\frac{\Delta\alpha}{\alpha})$  are well modeled by a Gaussian (or sine function) model with the same velocity standard deviation. Thus it seems that the error in  $\frac{\Delta\alpha}{\alpha}$  caused by this wavelength calibration is completely specified by just the standard deviation of the velocity offsets.

J.B.W. and K.G were supported in part by the U.S. Department of Energy under grant DE-FG03-97ER40546. MTM thanks the Australian

Research Council for a QEII Research Fellowship (DP0877998).

## REFERENCES

- Bahcall, J.N., Sargent, W.L.W., Schmidt, M. 1967, ApJ, 149, L11
- Butler, R.P., et al., 1996, PASP, 108, 500
- Chand, H., Srianand, R., Petitjean, P., Aracil, B., 2004, A&A, 417, 853
- D’Odorico, S., et al., 2000, Proc. SPIE, 4005, 121
- Griest, et al. 2010, ApJ 708, 158
- Levshakov, S.A., et al., 2007, A&A, 466, 1077
- Levshakov, S.A., et al., 2006, A&A, 449, 879
- Marcy, G. W., 2008, unpublished.
- Molaro, P., Reimers, D., Agafonova, I.I., & Levshakov, S.A., 2008, Eur. Phys. J. ST, 163, 173
- Murphy, M. T., et al., 2001a, MNRAS, 327, 1208
- Murphy, M. T., Webb, J. K., Flambaum, V. V., Churchill, C. W., Prochaska, J. X., 2001b, MNRAS, 327, 1236
- Murphy, M. T., Webb, J. K., and Flambaum, V. V., 2003, MNRAS, 345, 609
- Murphy, M. T., Webb, J. K., and Flambaum, V. V., 2004, VizieR Online Data Catalog, 734, 50609
- Murphy, M. T., Webb, J. K., and Flambaum, V. V., 2008, MNRAS, 384, 1053
- Murphy, M. T., Webb, J. K., and Flambaum, V. V., 2009, arXiv:0911.4512 (Memorie della Societa Astronomica Italiana (MmSAI), 80, 833)
- Osterbrock, D. E., et al., 2000, PASP, 112, 733
- Porsev, S.G., et al. , 2007, Phys. Rev. A 76, 052507
- Srianand, R., Chand, H., Petitjean, & P., Aracil, B., 2004, Phys. Rev. Let., 92, 121302
- Suzuki, N., et al. 2003, PASP, 115, 1050
- Varshalovich, D.A., Potekhin, A.Y., Ivanchik, A.V., 2000, in Dunford, R.W. et al. eds., AIP Conf. Proc. 506, X-Ray and Inner-Shell Processes, Argonne National Laboratory, Argonne, IL.

This 2-column preprint was prepared with the AAS L<sup>A</sup>T<sub>E</sub>X macros v5.2.

TABLE 2  
 MONTE CARLO RESULTS<sup>a</sup> FOR MEAN AND STANDARD DEVIATION OF  $\frac{\Delta\alpha}{\alpha}$

Exposure	$N_{\min}$	$\frac{\Delta\alpha}{\alpha}$	mean/ $10^{-6}$	$\sigma/10^{-6}$ for $N_{\text{sys}} = 1$	$\sigma/10^{-6}$ for $N_{\text{sys}} = 143$
1	2		1.74	41.6	3.57
1	4		0.53	5.21	0.443
1	6		-0.041	3.28	0.267
2	2		-1.68	44.7	3.74
2	4		0.330	6.41	0.540
2	6		0.297	3.36	0.279
3	2		1.02	58.9	4.83
3	4		0.706	6.67	0.548
3	6		0.245	3.43	0.280
Gaussian	2		-0.502	115	-
Gaussian	4		-0.080	11.2	-
Gaussian	6		-0.012	4.23	-
Sine	2		-1.78	104	-
Sine	4		-3.13	12.6	-
Sine	6		-0.308	4.64	-

<sup>a</sup>Only transitions within the iodine cell coverage are included from 200,000 realizations of  $N_{\text{sys}} = 1$ .

TABLE 3  
 STANDARD DEVIATION<sup>a</sup> OF  $\frac{\Delta\alpha}{\alpha}$  FROM WAVELENGTH CALIBRATION ERRORS AS A FUNCTION OF THE NUMBER OF TRANSITIONS.

$N_{\text{tran}}$	Percentage of realizations	Exposure 1: $\sigma/10^{-6}$	Gaussian: $\sigma/10^{-6}$
2	20.7%	228	91.4
3	29.7%	30.3	44.0
4	18.7%	8.61	11.2
5	11.7%	5.90	5.00
6	10.7%	3.34	4.17
7	6.3%	3.10	3.73
8	1.3%	3.36	3.60
9	1.0%	2.59	3.18

<sup>a</sup>For transitions that occur within the iodine cell coverage region of the spectrum, and for 200,000 realizations of  $N_{\text{sys}} = 1$

TABLE 4  
 MONTE CARLO RESULTS<sup>a</sup> FOR MEAN AND STANDARD DEVIATION OF  $\frac{\Delta\alpha}{\alpha}$

$N_{\min}$	Exposure 1: mean/ $10^{-6}$	Exposure 1: $\sigma/10^{-6}$	Gaussian: mean/ $10^{-6}$	Gaussian: $\sigma/10^{-6}$
2	-0.018	81.2	0.185	91.6
4	-0.101	4.99	-0.036	5.64
6	-0.064	2.59	-0.028	3.04
8	-0.051	2.00	-0.006	2.38
10	-0.042	1.71	-0.005	2.03
15	-0.029	1.30	0.004	1.59
20	0.153	1.05	0.007	1.35

<sup>a</sup>All of the 23 transitions falling between 3000Å and 10500Å are included (see text), for 200,000 realizations of  $N_{\text{sys}} = 1$ .